[3] A. Okaya and L. F. Barash, "The dielectric microwave resonator," *Proc. IRE*, vol. 50, pp. 2081–2092, Oct. 1962.
[4] J. L. Pellegrin, "The filling factor of shielded dielectric resonators," *IEEE Trans. Microwave Theory and Techniques*, vol. MTT-17, pp. 764–768, Oct. 1969.
[5] L. V. Alekseychik, V. M. Gevorkyan, and Yu A. Kazantzev, "Excitation of an open dielectric resonator in a transmission line," *Radiotekhnika i Elektronika*, vol. 17, pp. 1814–1821, Nov. 1972.
[6] R. E. Collin, *Foundations for Microwave Engineering*. New York: McGraw-Hill, 1966, pp. 183–190.
[7] ——, *Field Theory of Guided Waves*. New York: McGraw-Hill, 1960, pp. 224–232.
[8] R. F. Sohoo, *Theory and Applications of Ferrites*. Englewood Cliffs, NJ: Prentice-Hall, 1960, pp. 260–262.

Effect of Diode Parameters on Reflection-Type Phase Shifters

PRADEEP WAHI, STUDENT MEMBER, IEEE, AND K. C. GUPTA

Abstract—**This short paper describes effects of series inductance, shunt capacitance, and resistances associated with p-i-n diodes on the performance of reflection-type digital phase shifters using a shorted transmission line behind a shunt-mounted diode. It is found that the shunt capacitance is the most dominant reactance influencing the phase shift and it increases the phase-shift value. The series inductance reduces the phase-shift value. Expressions for phase shift in various cases are presented.**

Introduction

One of the design configurations for a reflection-type phase shifter consists of a p-i-n diode shunt mounted across a transmission line at a distance l from the shorted end [1]. Phase of the reflected wave at the diode plane changes when the bias on the diode is changed from forward to reverse, as the later implies inclusion of an additional line length l. Thus the phase shift obtained is given approximately by $2\beta l$ where β is the phase constant of the line. This arrangement is converted into a two-port phase shifter by using a circulator or a hybrid.

A simple procedure for designing such a phase shifter assumes the p-i-n diode to be ideal, i.e., short circuit when forward biased and open circuit when reverse biased. This method does not yield accurate result at higher frequencies when parasitic reactances and resistances associated with the diode become significant. This short paper describes the effect of diode reactances and resistances on the phase-shift characteristics of this type of phase shifter.

Diode Parameters

The important parameters of a p-i-n diode are; series inductance L (typically 0.4–2.0 nH), shunt capacitance C (0.1–2 pF), forward-bias series resistance R_s (0.5–2.0 Ω), and reverse-bias shunt resistance R ($\simeq$ 10 kΩ). The effect of these parameters may be considered analytically by taking them one by one in association with an ideal switch. Phase-shift and insertion-loss calculations are carried out by adding the diode admittance to the admittance of the line behind the diode and finding out the reflection coefficient caused by this combination.

Effect of Series Inductance

When an inductance L is in series with the ideal switch (Fig. 1 inset) the phase-shift expression is obtained as

$$\phi = 2\beta l + 2\tan^{-1}[\cot\beta l + Z_0/\omega L] - \pi. \tag{1}$$

Manuscript received February 3, 1975; revised January 26, 1976.
The authors are with the Advanced Centre for Electronic Systems, IIT, Kanpur, India.

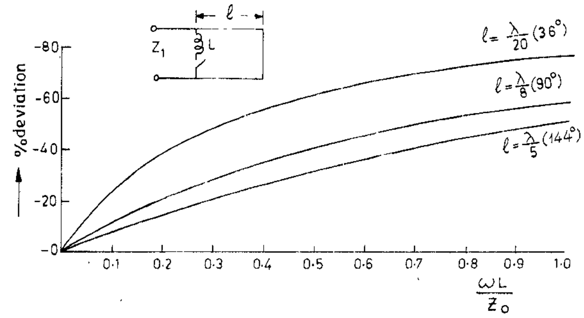

Fig. 1. Effect of series inductance L on the phase shift.

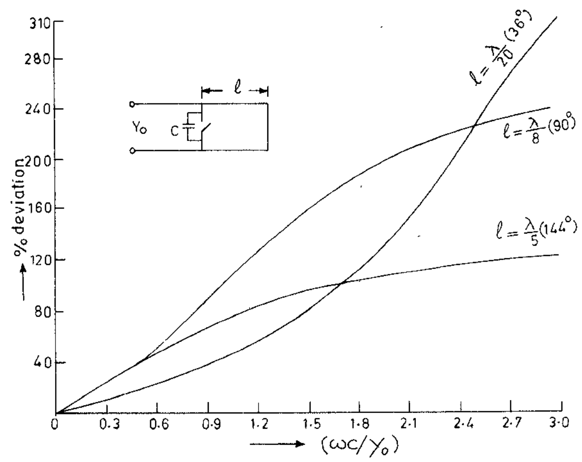

Fig. 2. Effect of shunt capacitance C on the phase shift.

It may be noted that the phase shift ϕ varies with both the line length behind the diode and the reciprocal of the normalized reactance ($Z_0/\omega L$). Differentiating (1) with respect to L one gets

$$\frac{\partial\phi}{\partial L} = \frac{2}{\left[1 + \left(\cot\beta l + \frac{Z_0}{\omega L}\right)^2\right]}\frac{Z_0}{\omega}\left(-\frac{1}{L^2}\right) \tag{2}$$

which shows that the phase shift decreases with an increase in L. The percentage deviation of the phase shift from an ideal case versus the normalized series reactance is plotted for three different cases in Fig. 1. It is seen that the deviation from the ideal case increases with the value of L. Also the deviation is higher for smaller values of phase shift (βl).

Effect of Shunt Capacitance

The expression for phase shift for the case when there is a capacitance in parallel with ideal switch (Fig. 2) is found to be

$$\phi = 2\tan^{-1}\left[\frac{\omega c}{Y_0} - \cot\beta l\right] - \pi. \tag{3}$$

The phase shift varies with both the length and the normalized shunt susceptance. Differentiating (3) with respect to capacitance C

$$\frac{\partial\phi}{\partial C} = \frac{1}{\left[1 + \left(\frac{\omega C}{Y_0} - \cot\beta l\right)^2\right]}\left(\frac{\omega}{Y_0}\right) \tag{4}$$

which is always positive. Hence the phase shift always increases with an increase in the capacitance value. The effect of increase

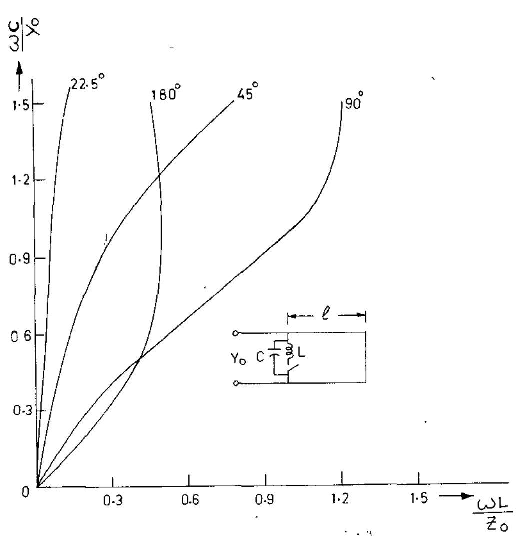

Fig. 3. Values of $\omega C/Y_0$ and $\omega L/Z_0$ for zero phase error for four values of phase shift.

in frequency on phase shift is similar to that of an increase in capacitance. Values of the phase shift deviation from an ideal case are plotted in Fig. 2 for three different cases. It is seen that the nature of this variation depends heavily upon the line length behind the diode. In general, the deviation decreases when $\beta\iota$ is increased.

Combined Effect of Series Inductance and Shunt Capacitance

When both the series inductance and shunt capacitance are present (Fig. 3), the phase-shift value in this case is given by

$$\phi = 2\tan^{-1}\left[\frac{\omega C}{Y_0} - \cot\beta\iota\right] - 2\tan^{-1}\left[\frac{\omega C}{Y_0} - \cot\beta\iota - \frac{Z_0}{\omega L}\right]. \quad (5)$$

Deviation from the ideal case reduces to zero for one value of line length behind the diode. This can be obtained by putting ϕ, (5), equal to $2\beta\iota$. The idea that inductance and capacitance of the diode can be selected to obtain no phase error was also mentioned in [1]. Fig. 3 presents a set of parameters, derived by using (5), which give zero phase error.

Effect of Series and Shunt Resistances

The expressions for the phase shift and the loss when there is a resistance in series with the ideal switch [Fig. 4(a)] are derived to be

$$\phi = \tan^{-1}\left[\frac{2\cot\beta\iota}{1-(G_s/Y_0)^2 - \cot^2\beta\iota}\right] \quad (6)$$

and

$$\text{loss} = 10\log\left[\frac{\{(1+G_s/Y_0)^2 + \cot^2\beta\iota\}^2}{\{1-(G_s/Y_0)^2 - \cot^2\beta\iota\}^2 + 4\cot^2\beta\iota}\right]\text{dB} \quad (7)$$

where $G_s = 1/R_s$.

Loss and percentage deviation (for $\beta\iota = \pi/4$) have been plotted in Fig. 4(a) as a function of R_s/Z_0. Phase-shift values do not deviate from the ideal case appreciably.

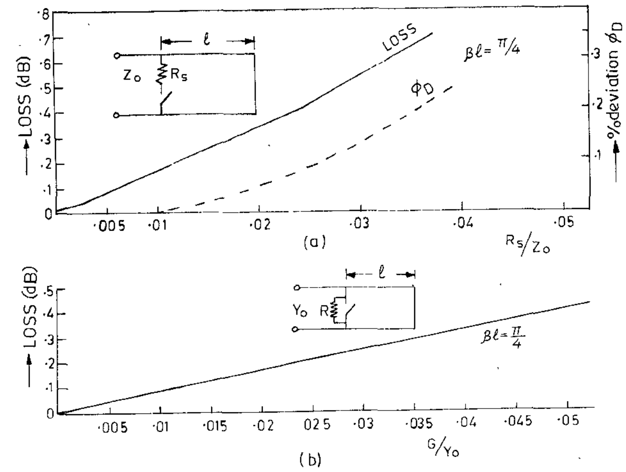

Fig. 4. (a) Variations of loss and phase shift with series resistance R_s. (b) Variation of loss with shunt resistance R.

For a shunt resistance R with an ideal switch [Fig. 4(b)], the expressions for the phase shift and loss are found out to be

$$\phi = -\tan^{-1}\left[\frac{2\cot\beta\iota}{1-(G/Y_0)^2 - \cot^2\beta\iota}\right] \quad (8)$$

and

$$\text{loss} = 20\log\left[1 + \frac{2(G/Y_0)}{1+\cot^2\beta\iota}\right]\text{dB} \quad (9)$$

where $G = 1/R$.

The results for loss versus G/Y_0 for $\beta\iota = \pi/4$ are shown in Fig. 4(b). As in the case of the series resistance, the loss is phase-shift dependent in this case also. The effect of G on phase shift is negligible (less than 0.01 percent).

Another important case is when both the series inductance and series resistance are present. In this case, the phase shift is given by

$$\phi = 2\beta\iota + \tan^{-1}\left[\frac{(\omega B'/Y_0) + \cot\beta\iota}{1 - G_s'/Y_0}\right] + \tan^{-1}\left[\frac{(\omega B'/Y_0) + \cot\beta\iota}{-(1+G_s'/Y_0)}\right] \quad (10)$$

where

$$G_s' = \frac{R_s}{R_s^2 + \omega^2 L^2}$$

and

$$B' = \frac{L}{R_s^2 + \omega^2 L^2}.$$

Usually, $\omega^2 L^2 \gg R_s^2$, and therefore $B' \simeq 1/(\omega^2 L)$ and $G_s' \simeq 0$. This reduces (11) to (1). Thus the phase-shift variation is similar to that in the case of only series inductance present with an ideal switch.

Concluding Remarks

The aforementioned results may be used to evaluate the order of error introduced by neglecting the reactances associated with p-i-n diodes. Some interesting observations emerging from this discussion are as follows.

1) Effects of series inductance and shunt capacitance depend upon normalized values of $\omega L/Z_0$ and $\omega C/Y_0$, respectively.

2) Series inductance decreases the value of phase shift, whereas shunt capacitance increases this value.

3) Shunt capacitance seems to be the most dominating reactance affecting the phase shift. This suggests that an arrangement which can vary shunt capacitance across the diode may be used for the adjustment of phase shift in the finally fabricated circuits.

4) Effects of the forward-bias and the reverse-bias resistances on phase shift are very small as compared to that of reactances.

References

[1] R. V. Garver, "Broad-band diode phase shifters," *IEEE Trans. Microwave Theory Tech.*, vol. MTT-20, pp. 314–323, May 1972.

Effects of the Surroundings on Electromagnetic-Power Absorption in Layered-Tissue Media

PAOLO BERNARDI, SENIOR MEMBER, IEEE, FRANCO GIANNINI, AND ROBERTO SORRENTINO

Abstract—**The influence of the surroundings on the interaction between electromagnetic (EM) waves and biological tissue is examined by schematizing the environment by a perfectly conducting screen placed beyond the irradiated tissue. The effects of standing waves, which are created in this situation, are determined as a function of the electrical and geometrical parameters of the structure. In particular, the hazard increase due to the presence of the screen combined with a phase disuniformity of the incident field—an elementary schematization of the "near-field"—is pointed out.**

I. Introduction

The use of equipment for industrial heating which uses electromagnetic (EM) energy has become more and more widespread in recent years. This apparatus generally operates at frequencies between 1 and 100 MHz with a power output of several hundreds of kilowatts [1]. Consequently, for the purpose of specifying a standard for protection against EM radiation, the interest in the phenomena of the interaction between EM waves and biological tissue has been extended also to this frequency range. In this approach, it has been necessary to reexamine several of the simplifying hypotheses generally valid at microwaves, but not sufficiently verified at lower frequencies [2]–[4]. In the microwave field, in fact, it is often possible to consider that the tissues are isotropic, that the radiating field can be schematized by a uniform plane wave, that the interaction takes place in free space, and that the tissues can be represented by models infinite in size. On the contrary, in the frequency range where the aforementioned equipment operates, the anisotropy of certain types of tissue should be taken into account; the interaction with man usually takes place in the radiative, or even reactive, "near-field" of the radiating equipment; the EM generator is often installed in an enclosed environment, usually consisting of industrial sheds; finally, the dimensions of the tissues play a part one cannot exclude from consideration. The usual approach to such complex problems consists in changing the aforementioned assumptions one at a time in such a way as to evaluate the influence of a single aspect of the phenomenon. In this way, the dependence of the absorbed power distribution on the curvature of the radiated surface and on the orientation of the body with respect to the incident plane-wave vector has been pointed out by adopting spherical and spheroidal models of the human body [5]–[7]. On the other hand, the influence of the anisotropy of the muscle on the absorbed-power distribution [8] and of the disuniformity of the field radiated by particular types of sources (e.g., the dipole with corner reflector [9] and the rectangular aperture with a given field distribution [10]) has been illustrated through the analysis of a single- or multiple-layered plane model.

The aim of the present work is to bring out, by the adoption of a plane model, the hitherto neglected influence of the surroundings on the interaction phenomena. In fact, the use of industrial heating equipment inside enclosed spaces in the presence of reflecting surfaces makes it impossible to consider the interaction as taking place in free space. The adoption of a plane model, besides making a substantial simplification of the analytical treatment, is justified since the phenomenon which can be thus brought out, can be more or less remarkable but not absent when one adopts a model more closely relevant to man or experimental animals in complex fields.

II. The Multilayered Model

The simplest schematization of the interaction between the EM field and biological tissue, in which account is taken of the environment, is shown in Fig. 1. Beyond a layered model, consisting of N biological tissues, and irradiated by a uniform plane-wave incident at angle θ, a perfectly conducting screen is placed at a distance d. Within each layer the field can be expressed as a superposition of a forward and reflected wave. From homogeneous Maxwell equations one obtains

$$\left.\begin{aligned} E_i^{\pm} &= \frac{H_{zi}^{\pm}}{j\omega\varepsilon_{ci}}\,[-j\beta_{0y}x_0 \pm k_{xi}y_0] + z_0E_{zi}^{\pm} \\ H_i^{\pm} &= \frac{E_{zi}^{\pm}}{j\omega\mu_0}\,[j\beta_{0y}x_0 \mp k_{xi}y_0] + z_0H_{zi}^{\pm} \end{aligned}\right\}\exp\,(\mp k_{xi}x - j\beta_{0y}y) \tag{1}$$

where ε_{ci} is the complex permittivity of the i layer and k_{xi} the complex propagation constant in the x direction; $\beta_{0y} = \omega\sqrt{\mu_0\varepsilon_0}\sin\theta$ is the phase constant in the y direction of the incident wave. The upper signs refer to the forward field and the lower signs to the reflected field, respectively. All the tissues are assumed to have the vacuum permeability μ_0. Given proper boundary conditions, it is possible to express the field in the i layer in terms of that in the $(i + 1)$ layer

$$\begin{aligned} E_{zi}^{\pm} = \frac{\pm 1}{2k_{xi}}\,[&E_{z(i+1)}^{+}(\pm k_{xi} + k_{x(i+1)}) \\ &\cdot \exp\,(\pm k_{xi} - k_{x(i+1)})d_i + E_{z(i+1)}^{-}(\pm k_{xi} - k_{x(i+1)}) \\ &\cdot \exp\,(\pm k_{xi} + k_{x(i+1)})d_i] \end{aligned}$$

$$\begin{aligned} H_{zi}^{\pm} = \frac{\pm\varepsilon_{ci}}{2k_{xi}}\Bigg[&H_{z(i+1)}^{+}\left(\pm\frac{k_{xi}}{\varepsilon_{ci}} - \frac{k_{x(i+1)}}{\varepsilon_{c(i+1)}}\right) \\ &\cdot \exp\,(\pm k_{xi} - k_{x(i+1)})d_i + H_{z(i+1)}^{-}\left(\frac{\pm k_{xi}}{\varepsilon_{ci}} + \frac{k_{x(i+1)}}{\varepsilon_{c(i+1)}}\right) \\ &\cdot \exp\,(\pm k_{xi} + k_{x(i+1)})d_i\Bigg] \end{aligned}$$

Manuscript received November 11, 1975; revised January 27, 1976. This work was partially supported by the Consiglio Nazionale delle Ricerche, Italy.

The authors are with the Institute of Electronics, University of Rome, Rome, Italy.